



Contents lists available at ScienceDirect

# Spectrochimica Acta Part A: Molecular and Biomolecular Spectroscopy

journal homepage: [www.elsevier.com/locate/saa](http://www.elsevier.com/locate/saa)

## Syntheses, spectroscopic characterization, thermal study, molecular modeling, and biological evaluation of novel Schiff's base benzil bis(5-amino-1,3,4-thiadiazole-2-thiol) with Ni(II), and Cu(II) metal complexes

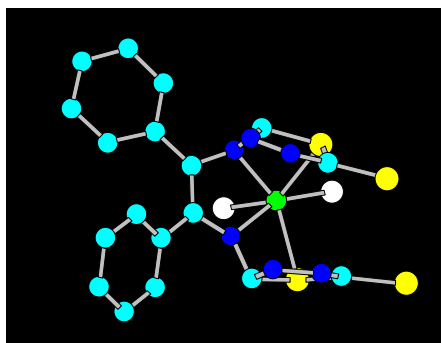
Sulekh Chandra<sup>a,\*</sup>, Seema Gautam<sup>a</sup>, Hament Kumar Rajor<sup>b</sup>, Rohit Bhatia<sup>c</sup><sup>a</sup> Department of Chemistry, Zakir Husain Delhi College, University of Delhi, JLN Marg, New Delhi 110002, India<sup>b</sup> Department of Chemistry, Ramjas College, University of Delhi, New Delhi 110007, India<sup>c</sup> University of Delhi, New Delhi 110007, India

### HIGHLIGHTS

- Synthesis, characterization and Molecular modeling of novel Schiff's base ligand and complexes.
- Complexes possessed octahedral, tetragonal, square pyramidal, and tetrahedral geometry.
- Thermal data suggested that metal complexes were more stable than free ligand.
- *In vitro* antimicrobial activity of ligand and its complexes were screened.
- Complexes were found more biologically sensitive than ligand.

### GRAPHICAL ABSTRACT

Synthesized ligand behaves as tetradentate and coordinates to metal ion through sulfur atoms of thiol ring and nitrogen atoms of imine group. Ni(II), and Cu(II) complexes were synthesized with this nitrogen–sulfur donor (N<sub>2</sub>S<sub>2</sub>) ligand. Geometry optimized structure of [Cu(L)Cl<sub>2</sub>] complex.



### ARTICLE INFO

#### Article history:

Received 24 February 2014

Received in revised form 1 July 2014

Accepted 24 August 2014

Available online 3 September 2014

#### Keywords:

Schiff's bases  
Metal complexes  
Molecular modeling  
Spectral studies  
Biological evaluation

### ABSTRACT

Novel Schiff's base ligand, benzil bis(5-amino-1,3,4-thiadiazole-2-thiol) was synthesized by the condensation of benzil and 5-amino-1,3,4-thiadiazole-2-thiol in 1:2 ratio. The structure of ligand was determined on the basis of elemental analyses, IR, <sup>1</sup>H NMR, mass, and molecular modeling studies. Synthesized ligand behaved as tetradentate and coordinated to metal ion through sulfur atoms of thiol ring and nitrogen atoms of imine group. Ni(II), and Cu(II) complexes were synthesized with this nitrogen–sulfur donor (N<sub>2</sub>S<sub>2</sub>) ligand. Metal complexes were characterized by elemental analyses, molar conductance, magnetic susceptibility measurements, IR, electronic spectra, EPR, thermal, and molecular modeling studies. All the complexes showed molar conductance corresponding to non-electrolytic nature, expect [Ni(L)](NO<sub>3</sub>)<sub>2</sub> complex, which was 1:2 electrolyte in nature. [Cu(L)(SO<sub>4</sub>)] complex may possessed square pyramidal geometry, [Ni(L)](NO<sub>3</sub>)<sub>2</sub> complex tetrahedral and rest of the complexes six coordinated octahedral/tetragonal geometry. Newly synthesized ligand and its metal complexes were examined against the opportunistic pathogens. Results suggested that metal complexes were more biological sensitive than free ligand.

© 2014 Elsevier B.V. All rights reserved.

\* Corresponding author. Tel.: +91 9811226273.

E-mail address: [schandra\\_00@yahoo.com](mailto:schandra_00@yahoo.com) (S. Chandra).

## Introduction

Schiff's bases and their transition metal complexes were playing an important role in the development of coordination chemistry [1,2]. Schiff's base metal complexes were studied extensively because of their attractive chemical and physical properties and their wide range of applications in numerous scientific areas [3]. Schiff's bases had a chelating structure and were in demand because they were straight forward to prepare [4]. In Azomethine derivatives, the C=N linkage was essential for biological activities like antifungal [5], antibacterial [6], antitumour [7], antimalarial [8], antiviral [9,10], etc. The synthesis of Schiff's base ligand incorporating 1,3,4-thiadiazole ring as amine was attracted widespread attention due to their diverse pharmacological properties such as antimicrobial, analgesic, and anti-hepatitis B viral activities [11]. Thiadiazole derived Schiff's bases showed analgesic, and inflammatory activities also [12]. In recent years, a number of research articles had been published on transition metal complexes derived from 5-amino-1,3,4-thiadiazole-2-thiol and its derivatives which contain aza, oxo-aza, and thio-aza donor atoms [13,14]. The present report deals with synthesis, spectroscopic characterization, thermal study, and biological evaluation of Ni(II), and Cu(II) complexes with tetradentate ligand, which was derived from benzil and 5-amino-1,3,4-thiadiazole-2-thiol.

## Experimental details

### Materials

All chemicals used were commercial products and used as supplied. 5-Amino-1,3,4-thiadiazole-2-thiol, and benzil were of AR grade and procured from Alfa Aesar, Heysham, England and Sigma Aldrich, Bangalore, India. Metal salts were purchased from E. Merck, India and were used as received. All used solvents were of spectroscopic grade.

### Synthesis of Schiff's base ligand

An ethanolic solution of 5-amino-1,3,4-thiadiazole-2-thiol (2 mol, 2.664 g) was heated for 15 min. and then added to hot ethanolic solution of benzil (1 mol, 2.102 g) with continuous stirring and the reaction solution was refluxed for 5 h at 60 °C. It was allowed to stay at room temperature and kept in refrigerator overnight. On cooling, the yellow color solid product was precipitated out. It was filtered off, washed several times with cold ethanol, distilled water and then dried in vacuum over P<sub>4</sub>O<sub>10</sub>. Synthesis of ligand is given in Scheme 1 (Supplementary Material).

### Synthesis of metal complexes

A hot ethanolic solution of the corresponding metal salt, (except sulfate which was taken in aqueous medium) (0.001 mol) was mixed with hot ethanolic solution of Schiff's base ligand (0.001 mol) and content refluxed for 10–12 h at temp. 85–90 °C. pH (5–7) was adjusted by adding of 2–3 drops of aqueous ammonia. The corresponding colored complexes were separated out by filtration, washed thoroughly with ethanol, distilled water and dried under vacuum over P<sub>4</sub>O<sub>10</sub>.

### Analytical and physical measurements

Elemental study (CHN) was analyzed on Carlo-Erba 1106 elemental analyzer. Molar conductance was measured on the ELICO (CM82T) conductivity bridge. Magnetic susceptibilities were measured at room temperature on a Gouy balance using CuSO<sub>4</sub>·5H<sub>2</sub>O as

calibrant. IR spectra were recorded on FT-IR spectrum BX-II spectrophotometer in Csl pellet. The electronic spectra were recorded in DMSO on Shimadzu UV-visible mini-1240 spectrophotometer. Electronic impact mass spectrum was recorded on JEOL, JMS-DX-303 mass spectrometer. <sup>1</sup>H NMR spectra was recorded on a Bruker Advanced DPX-300 spectrometer using DMSO-d<sub>6</sub> as a solvent at IIT Delhi. EPR spectra of all complexes were recorded at room temperature (RT) on E<sub>4</sub>-EPR spectrometer using the DDPH as the g-marker at SAIF, IIT Bombay. Thermo gravimetric analysis was carried out in dynamic nitrogen atmosphere (30 mL/min) with a heating rate of 10 °C/min using a Shimadzu TGA-50H thermal analyzer. Molecular modeling of ligand and its metal complexes was performed using Hyperchem. 7.51 version.

### Molecular modeling

3D molecular modeling of the proposed structure of ligand and its metal complexes was performed using Hyperchem. 7.51 version. This version was used to calculate energy and other parameters like bond angles, bond lengths by Molecular Mechanics, MM plus force field. Hydrogen atoms were omitted for the sake of clarity. The correct stereochemistry was assured through the manipulation and modification of the molecular coordinates to obtain reasonable low energy molecular geometries. Several cycles of energy minimization had to be carried for each molecule. Vibration analysis was done to check the absence of imaginary frequencies.

### Antibacterial screening

The antibacterial screening of ligand and its metal complexes was tested against some bacteria *Escherichia coli*, *Staphylococcus aureus*, *Pseudomonas aeruginosa*, and *Klebsiella pneumonia* by using paper disk diffusion method [15]. Base plates were prepared by pouring 10 mL of autoclaved Muller Hinton agar into sterilized Petri dishes (9 mm diameter) and allowing them to settle. Molten autoclaved Muller Hinton that was kept at 38 °C was incubated with a broth culture of used bacteria species. Prepared plates were incubated for 24–30 h and the inhibition zones (mm) were measured around each disk carefully. As organism grows, it forms a turbid layer, except in the region where the concentration of antibacterial agent was above the minimum inhibitory concentration, and a zone of inhibition was seen. The solutions of tested compounds were prepared in DMSO.

### Antifungal screening

The Poison food Technique was applied to examine fungicidal investigations of synthesized ligand and its metal complexes against some fungi *Rhizoctonia solani*, *Sclerotium rolfsii*, *Macrophomina phaseolina*, *Fusarium oxysporum*, and *Aspergillus niger*. DMSO and Fluconazole were employed as a control and standard fungicide, respectively. The inhibition of the mycelial growth of fungi was expressed in percentage and determined from the growth in the test plate relative to the respective control plate as given below:

$$I(\%) = (CT)/C \times 100,$$

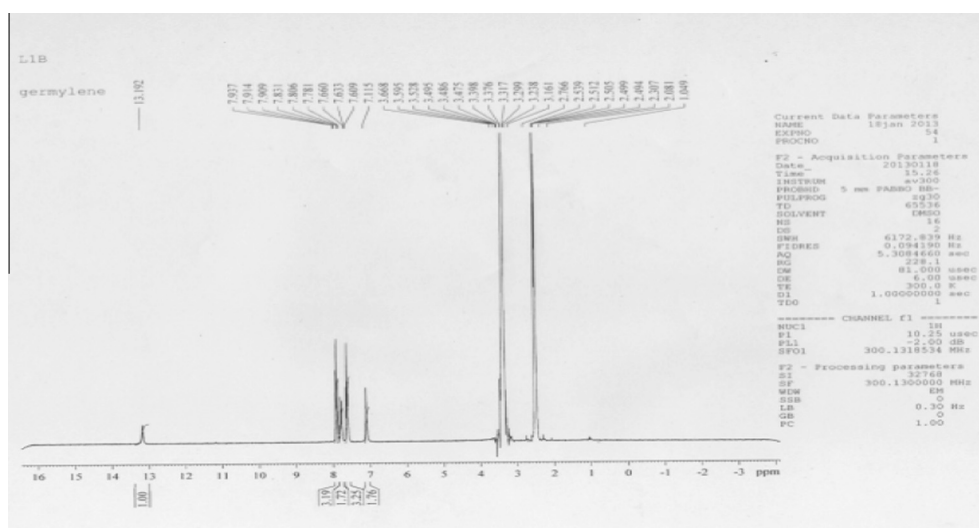
where I = % Inhibition, C = Radial diameters of the colony in control, T = Radial diameter of the colony in test compound.

## Results and discussion

Metal complexes were synthesized by mixing the hot ethanolic solution of ligand with ethanolic solution of the corresponding metal salt in 1:1 ratio. The Schiff's base ligand behaved as a

**Table 1**  
Molar conductance and elemental analyses of the ligand and its metal complexes.

Compound	Mol. Wt.	pH	Molar conductance ( $\Omega^{-1} \text{ cm}^2 \text{ mol}^{-1}$ )	Color	Yield (%)	Melting point ( $^{\circ}\text{C}$ )	Elemental analyses (%) found (calculated)			
							M	C	H	N
Ligand(L)	440	6	–	Light	68	80	–	49.09	2.72	19.09
$\text{C}_{18}\text{H}_{12}\text{N}_6\text{S}_4$				Yellow				(49.5)	(2.70)	(19.7)
$[\text{Ni}(\text{L})\text{Cl}_2]$	569.7	5	20	Mehendi	60	>250	10.30	37.91	2.10	14.74
$\text{C}_{18}\text{H}_{12}\text{N}_6\text{S}_4\text{Cl}_2\text{Ni}$							(10.38)	(37.95)	(2.02)	(14.69)
$[\text{Ni}(\text{L})](\text{NO}_3)_2$	628.7	7	173	Parrot	62	>250	9.33	34.35	1.90	17.81
$\text{C}_{18}\text{H}_{12}\text{N}_8\text{S}_4\text{O}_6\text{Ni}$				Green			(9.30)	(34.35)	(1.95)	(17.79)
$[\text{Cu}(\text{L})\text{Cl}_2]$	574.5	6	18	Mehendi	65	>250	11.05	37.59	2.08	14.62
$\text{C}_{18}\text{H}_{12}\text{N}_6\text{S}_4\text{Cl}_2\text{Cu}$				Green			(11.09)	(37.62)	(2.04)	(14.66)
$[\text{Cu}(\text{L})](\text{NO}_3)_2$	633.5	6	21	Green	65	>250	10.02	34.09	1.89	17.67
$\text{C}_{18}\text{H}_{12}\text{N}_8\text{S}_4\text{O}_6\text{Cu}$				Green			(10.00)	(34.10)	(1.88)	(17.66)
$[\text{Cu}(\text{L})](\text{SO}_4)$	599.5	5	15	Green	62	>250	9.13	31.05	1.72	12.07
$\text{C}_{18}\text{H}_{12}\text{N}_6\text{S}_5\text{O}_4\text{Cu}$							(10.01)	(31.05)	(1.75)	(12.09)

**Fig. 1.**  $^1\text{H}$  NMR spectrum of Schiff's base ligand.

tetradentate ligand and coordinated to metal ion through nitrogen of imine and sulfur of thiazole ring. All complexes were soluble in DMSO. The molar conductance value of nitrate complex of Ni(II), and for other complexes were 173, and  $10\text{--}22 \Omega^{-1} \text{ cm}^2 \text{ mol}^{-1}$  respectively. These values were corresponded to electrolytic and non-electrolytic nature of the complexes. Thus the complexes may be formulated as  $[\text{Ni}(\text{L})](\text{NO}_3)_2$  and  $[\text{M}(\text{L})\text{X}_2]$  (where  $\text{M} = \text{Ni}(\text{II}), \text{Cu}(\text{II}), \text{L} = \text{Schiff's base ligand}$ , and  $\text{X} = \text{Cl}^-, \text{NO}_3^-, \frac{1}{2} \text{SO}_4^{2-}$ ). The analytical data of ligand and its metal complexes, together with their physical properties is given in Table 1.

#### $^1\text{H}$ NMR spectrum of ligand

$^1\text{H}$  NMR spectrum of Schiff's base ligand [benzil bis(5-amino-1,3,4-thiadiazole-2-thiol)] in  $\text{DMSO-}d_6$  exhibited following signals:  $\delta$  7.78–7.93 ppm (8H, m, Ar–H),  $\delta$  3.34 ppm (1H, s, SH) Fig. 1. These signals indicate that two different types of proton are present in ligand.

#### Mass spectrum

The electronic impact mass spectrum of the Schiff's base ligand confirmed the proposed formula by showing a molecular ion peak at  $m/z = 439$ , corresponds to species  $[\text{C}_{18}\text{H}_{11}\text{N}_6\text{S}_4]^+$ . It also showed a series of peaks i.e. 407, 323, 220, 117, and 84 corresponding to

various fragments. These peaks (407, 323, 220, 117, and 84) appeared to loss of following species ( $-\text{S}$ ), ( $-\text{C}_2\text{N}_2\text{S}$ ), ( $-\text{C}_7\text{H}_5\text{S}$ ), ( $-\text{C}_7\text{H}_5\text{N}$ ), and (SH) respectively. The intensity of these peaks gave an idea of the stabilities of fragments. The fragmentation path of the ligand is given in Fig. 2 (Supplementary Material).

#### IR spectra

The important IR bands of ligand and metal complexes along with their assignment are given in Table 2. The IR spectrum of free ligand displayed bands in the region  $3190\text{--}3010 \text{ cm}^{-1}$ ,  $1618 \text{ cm}^{-1}$ ,  $795 \text{ cm}^{-1}$ , and  $3500\text{--}3350 \text{ cm}^{-1}$  corresponding to the presence of the aromatic C–H stretching, azomethine group (C=N), stretching vibration of C=S group, and SH stretching vibration Fig. 3(a). On complex formation, bands at  $1618 \text{ cm}^{-1}$ , and  $795 \text{ cm}^{-1}$ , shifted downward, which suggested that coordination take place through nitrogen atom of azomethine, and sulfur atom of thiazole ring [16]. This binding of the ligand to metal ion was also supported by the appearance of new IR bands at  $405\text{--}428 \text{ cm}^{-1}$  and  $305\text{--}32 \text{ cm}^{-1}$  due to  $\nu(\text{M}\text{--}\text{N})$  and  $\nu(\text{M}\text{--}\text{S})$  vibrations, respectively. This discussion revealed that the Schiff's base ligand coordinates to metal ions as tetradentate chelate to form complexes. However, a strong absorption band at about  $3350\text{--}3500 \text{ cm}^{-1}$  remained as such in IR spectra of metal complexes, indicated that SH do not coordinate to metal ion.

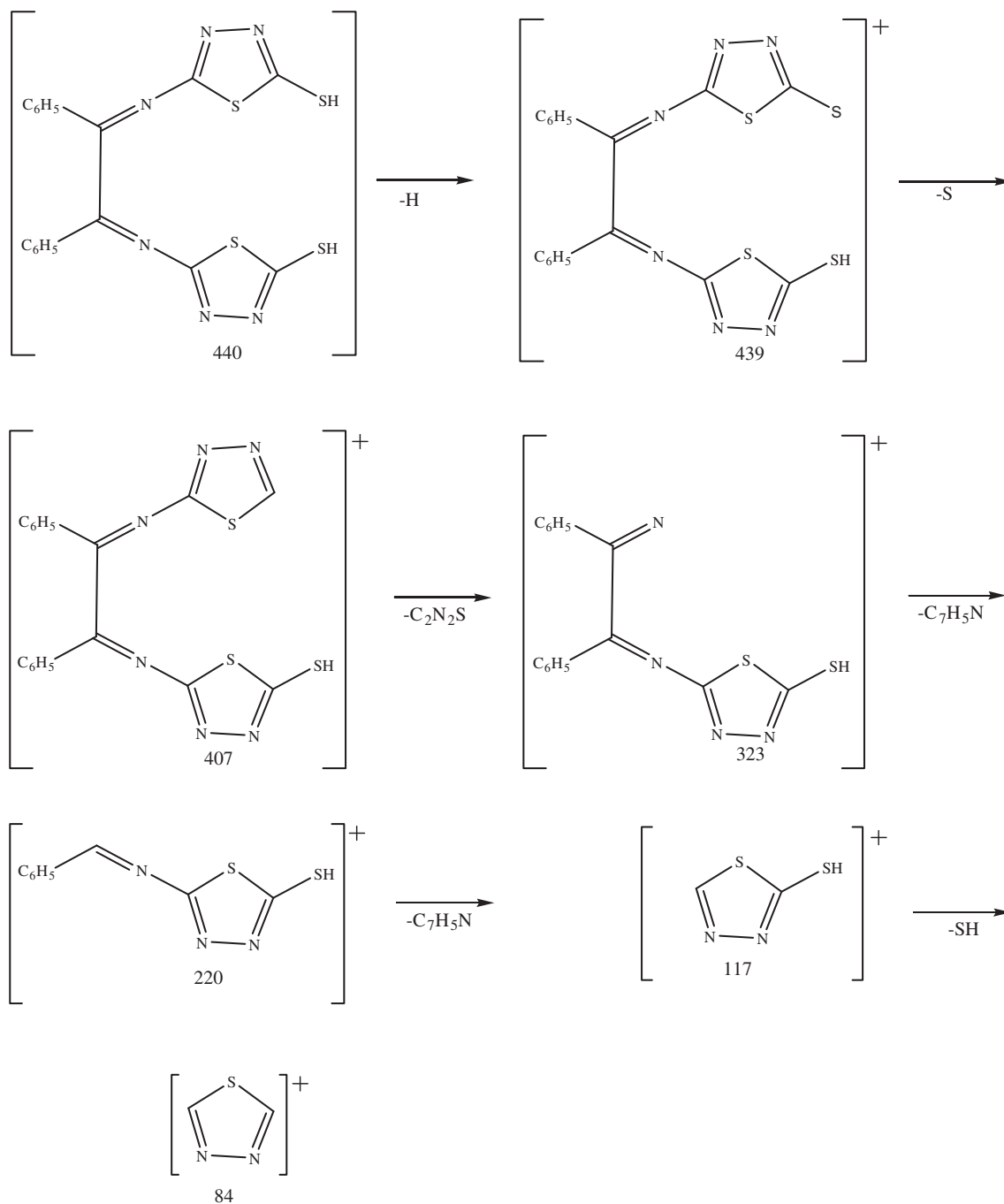
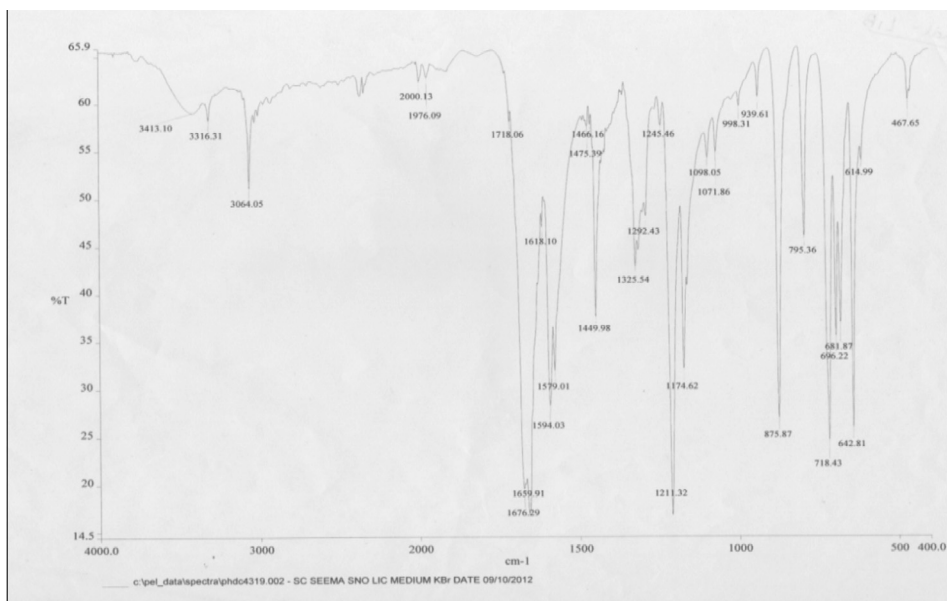


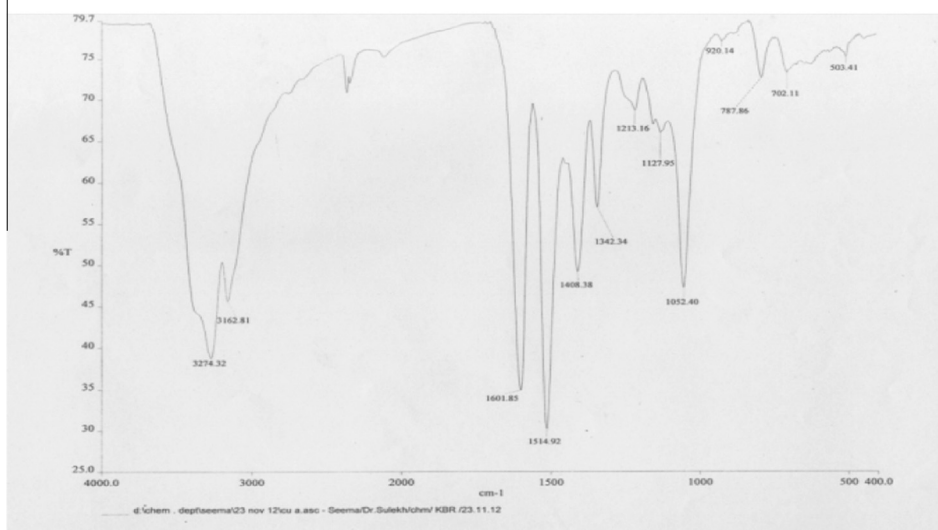
Fig. 2. Mass fragmentation of Schiff's base ligand.

**Table 2**  
Characteristic IR bands ( $\text{cm}^{-1}$ ) of Schiff's base and its metal complexes.

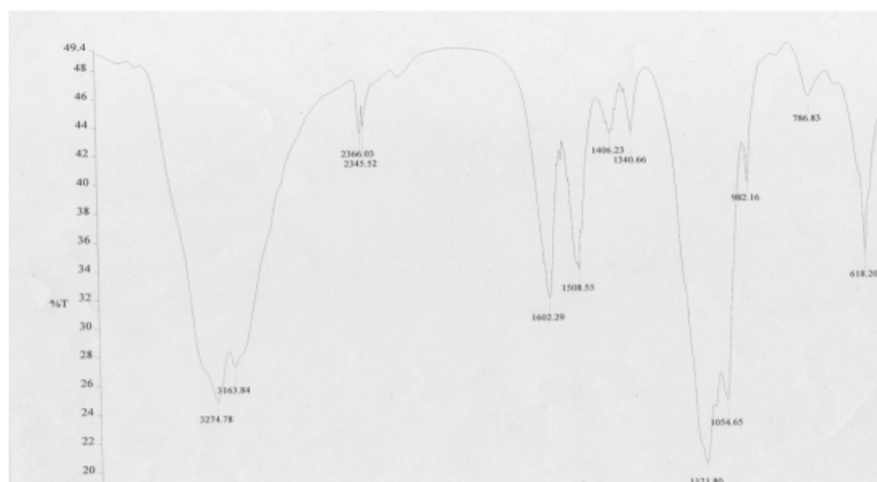
Compound	Assignments				Bands due to anions
	$\nu$ (C=N)	$\nu$ (C=S)	$\nu$ (C-H)Ar	$\nu$ (S-H)	
Ligand(L)	1594	795	3064	2500	
[Ni(L)Cl <sub>2</sub> ]	1522	770	3179	2500	Band observed at 345–325 $\text{cm}^{-1}$ indicating the presence of M–Cl bond
[Ni(L)](NO <sub>3</sub> ) <sub>2</sub>	1522	770	3153	2500	Band appeared at 1384 $\text{cm}^{-1}$ indicating uncoordinated nature of nitrate group [17]
[Cu(L)Cl <sub>2</sub> ]	1514	787	3162	2500	Band observed at 345–325 $\text{cm}^{-1}$ indicating the presence of M–Cl bond
[Cu(L)(NO <sub>3</sub> ) <sub>2</sub> ]	1490	778	3163	2500	$\nu_5 = 1410 \text{ cm}^{-1}$ , $\nu_1 = 1320 \text{ cm}^{-1}$ , $\nu_2 = 1021 \text{ cm}^{-1}$ and $\Delta(\nu_5 - \nu_1) = 104 \text{ cm}^{-1}$ indicating unidentate nature of nitrate group
[Cu(L)(SO <sub>4</sub> )]	1508	786	3163	2500	$\nu_3$ Splitting at 1121 $\text{cm}^{-1}$ and 1054 $\text{cm}^{-1}$ indicating the unidentate nature of sulfate group [18]



(a)



(b)



(c)

**Fig. 3.** IR spectrum (a) Schiff's base Ligand, (b) [Cu(L)Cl<sub>2</sub>] and (c) [Cu(L)(SO<sub>4</sub>)].

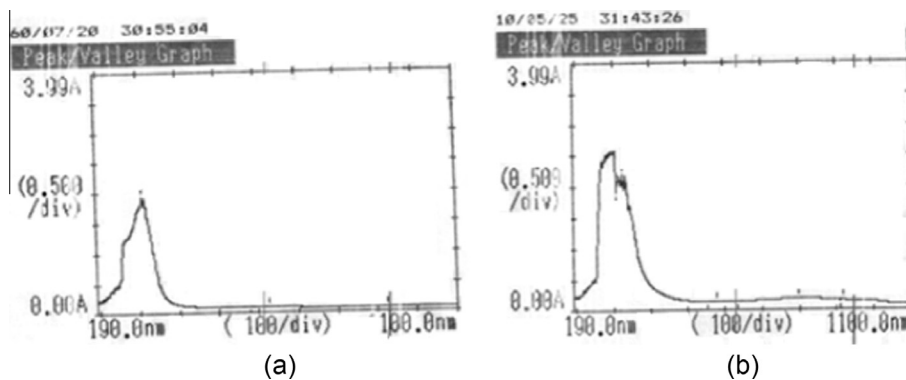


Fig. 4. UV-visible spectra of (a) [Ni(L)](NO<sub>3</sub>)<sub>2</sub> and (b) [Cu(L)(SO<sub>4</sub>)].

**Table 3**  
EPR spectral data of the Cu(II) complexes.

Complex	$g_{  }$	$g_{\perp}$	$g_{iso}$	$g_1$	$g_2$	$g_3$	$R$	$G$
[Cu(L)Cl <sub>2</sub> ]	2.34	2.09	2.09	–	–	–	–	3.7
[Cu(L)(NO <sub>3</sub> ) <sub>2</sub> ]	2.58	2.05	2.1	–	–	–	–	3.1
[Cu(L)(SO <sub>4</sub> )]	–	–	2.16	2.09	2.13	2.27	0.28	–

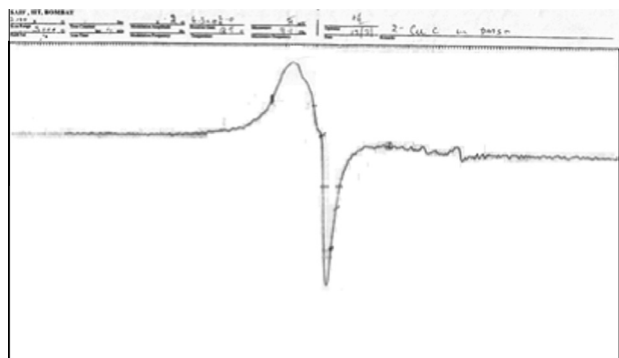


Fig. 5. EPR spectrum of [Cu(L)(SO<sub>4</sub>)].

#### Bands due to anion

In IR spectra of chloride complexes, bands corresponding to (M–Cl) were observed at 345–325 cm<sup>-1</sup> Fig. 3(b). The IR spectrum of the nitrate complex of Ni(II) showed a strong band at 1384 cm<sup>-1</sup> corresponds to uncoordinated behavior of nitrate ion. Spectrum of sulfate complex of Cu(II) showed that band  $\nu_3$  splitted at 1121 cm<sup>-1</sup> and 1054 cm<sup>-1</sup>, corresponded to unidentate behavior of sulfate ion Fig. 3(c).

#### Electronic spectra and magnetic moments

##### Nickel(II) complexes

The magnetic moments of Ni(II) complexes lies in the range 2.96–2.98 BM. These values indicated the presence of two unpaired

**Table 4**  
Electronic spectral bands (cm<sup>-1</sup>) and ligand field parameters of the complexes.

Complexes	$\lambda_{max}$ (cm <sup>-1</sup> )	$\mu_{eff}$ (BM)	Dq (cm <sup>-1</sup> )	$B$ (cm <sup>-1</sup> )	$\beta$	$\nu_2/\nu_1$	LFSE (kJ mol <sup>-1</sup> )
[Ni(L)Cl <sub>2</sub> ]	10101, 15432, 29498	2.96	1010	975	0.93	1.52	144
[Ni(L)](NO <sub>3</sub> ) <sub>2</sub>	9050, 15000, 22500	2.97	905	690	0.66	1.65	152
[Cu(L)Cl <sub>2</sub> ]	9569, 18621, 35335	1.88	–	–	–	–	–
[Cu(L)(NO <sub>3</sub> ) <sub>2</sub> ]	9680, 18621, 36900	1.96	–	–	–	–	–
[Cu(L)(SO <sub>4</sub> )]	11709, 18621, 36101	1.92	–	–	–	–	–

electrons. The electronic spectra of the [Ni(L)Cl<sub>2</sub>] complex showed bands in the range 9661–10,834, 11,223–18,621, and 21,739–32,573 cm<sup>-1</sup> and may be assigned to the <sup>3</sup>A<sub>2g</sub>(F) → <sup>3</sup>T<sub>2g</sub>(F), <sup>3</sup>A<sub>2g</sub>(F) → <sup>3</sup>T<sub>1g</sub>(F) and <sup>3</sup>A<sub>2g</sub>(F) → <sup>3</sup>T<sub>1g</sub>(P) transitions, respectively, characteristic to an octahedral geometry [19]. The electronic spectra of the [Ni(L)](NO<sub>3</sub>)<sub>2</sub> complex showed three bands in range of 9000–10,000, 10,000–15,000, and 15,000–25,000 cm<sup>-1</sup> these transition correspond to tetrahedral geometry Fig. 4(a) [20].

##### Copper(II) complexes

The value of magnetic moment indicated the presence of one unpaired electron (1.88–2.01 BM). In electronic spectrum of chloro, and nitrate complexes of Cu(II), bands appeared in the range of 9569–12,515 cm<sup>-1</sup>, and 18,245–20,450 cm<sup>-1</sup> may be assigned to the transitions, <sup>2</sup>B<sub>1g</sub> → <sup>2</sup>A<sub>1g</sub>( $\nu_1$ ), <sup>2</sup>B<sub>1g</sub> → <sup>2</sup>B<sub>2g</sub>( $\nu_2$ ) respectively. The third band at 30,769–37,174 cm<sup>-1</sup> may be due to charge transfer. Therefore, the complexes may be considered to possess a tetragonal geometry [21,22]. The electronic spectrum of the sulfate complex showed bands at 11,709 cm<sup>-1</sup>, 18,621 cm<sup>-1</sup> and third band at 36,101 cm<sup>-1</sup>. Third band was appeared due to charge transfer Fig. 4(b). Thus complex may possess either square-pyramidal or trigonal bipyramidal geometry.

##### Electronic paramagnetic resonance spectra

EPR spectra of Cu(II) complexes were recorded at room temperature as polycrystalline sample, on X band at frequency of 9.1 GHz under the magnetic-field strength of 3000G. The analysis of EPR spectrum of complexes gave the value of  $g_{||}$  (2.34–2.58) and  $g_{\perp}$  (1.70–2.09) Table 3. The trend  $g_{||} > g_{\perp} > 2.0023$ , was observed, indicated that the unpaired electron was localized in the  $d_{x^2-y^2}$ , orbital of the Cu(II) ion. Thus tetragonal geometry was confirmed for the aforesaid complexes. The geometric parameter  $G$  was evaluated by using the following relation  $G = (g_{||} - 2)/(g_{\perp} - 2)$ , which measures the exchange interaction between the metal centers. If  $G$  is greater than 4, the exchange interaction was negligible or  $G$  is less than 4 indicate considerable exchange interaction in the solid complexes. [23]. The  $G$  value was found less than 4; it suggested that there was exchange interaction in solid complexes. The IR spectrum of [Cu(L)(SO<sub>4</sub>)] complex suggested five coordinated geometry. Two

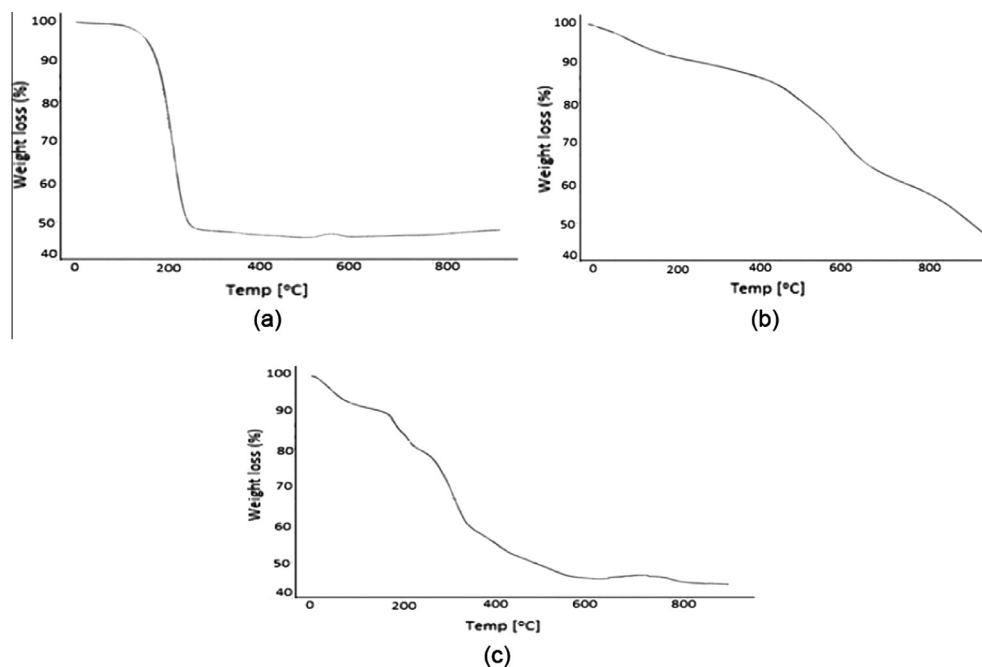


Fig. 6. TGA spectra of (a) Schiff's base ligand, (b) [Ni(L)Cl<sub>2</sub>] and (c) [Cu(L)Cl<sub>2</sub>].

Table 5

Thermal data for the ligand and its complexes.

Compound	Temperature range (°C)	TG weight loss (%)		Assignments
		Calc (%)	Found (%)	
[Ni(L)Cl <sub>2</sub> ]	25–230	12.46	12.45	–Cl <sub>2</sub>
	230–495	31.24	31.20	–C <sub>14</sub> H <sub>10</sub>
	495–780	45.98	45.99	C <sub>4</sub> H <sub>2</sub> N <sub>6</sub> S <sub>4</sub> Ni
[Ni(L)](NO <sub>3</sub> ) <sub>2</sub>	25–270	19.93	19.91	–(NO <sub>3</sub> ) <sub>2</sub>
	270–510	28.61	28.60	–C <sub>14</sub> H <sub>10</sub>
	510–750	36.97	36.99	–C <sub>4</sub> H <sub>2</sub> N <sub>6</sub> S <sub>3</sub>
[Cu(L)Cl <sub>2</sub> ]	25–220	12.35	12.28	–Cl <sub>2</sub>
	220–480	30.98	30.90	–C <sub>14</sub> H <sub>10</sub>
	480–755	40.03	40.00	C <sub>4</sub> H <sub>2</sub> N <sub>6</sub> S <sub>3</sub> CuS
[Cu(L)](NO <sub>3</sub> ) <sub>2</sub>	25–280	19.8	19.8	–(NO <sub>3</sub> ) <sub>2</sub>
	280–508	28.38	28.39	–C <sub>14</sub> H <sub>10</sub>
	508–750	41.78	41.76	–C <sub>4</sub> H <sub>2</sub> N <sub>6</sub> S <sub>4</sub> Cu
[Cu(L)](SO <sub>4</sub> )	25–240	13.34	13.33	–SO <sub>4</sub>
	240–510	29.69	29.65	–C <sub>14</sub> H <sub>10</sub>
	510–780	43.70	43.71	–C <sub>4</sub> H <sub>2</sub> N <sub>6</sub> S <sub>4</sub> CuO

basic structures were possible for five coordinated geometry i.e. trigonal bipyramidal or square pyramidal, which were characterized by the ground states  $d_{x^2-y^2}$  or  $d_z^2$ , respectively. EPR spectrum of this complex provided an excellent basis for distinguishing between these two ground states. For this system, parameter  $R$  is calculated [ $R = (g_2 - g_1)/(g_3 - g_2)$ ]. If the value of ' $R$ ' is greater than one, ground state is predominantly to  $d_z^2$ . On the other hand, the value of ' $R$ ' is less than one, the ground state is predominantly to  $d_{x^2-y^2}$ . EPR spectrum of the [Cu(L)(SO<sub>4</sub>)] complex shows three  $g$  values. The values of  $g_1$ ,  $g_2$ ,  $g_3$ , and  $R$  were 2.09, 2.13, 2.27, and 0.28 respectively. As the value of ' $R$ ' was less than one, ground state was predominantly  $d_{x^2-y^2}$  which was consistent with a square pyramidal geometry Fig. 5 [24].

#### Ligand field parameters

Various ligand field parameters i.e.  $Dq$ ,  $B$  and  $\beta$ , for the complexes were calculated [25]. The value of  $Dq$ , and  $B$  were calculated by using first and third transitions. The calculated parameters were given in Table 4. The nephelauxetic parameter  $\beta$  was obtained by using the relation:  $\beta = B(\text{complex})/B(\text{free-ion})$ , where  $B$  was the Racah inter-electronic repulsion parameter, and the value of  $B$  (free ion) for Ni(II) is  $1041 \text{ cm}^{-1}$ . The values of  $\beta$  are 0.93 and 0.66. These values indicated the covalent character in metal ligand ' $\sigma$ ' bond.

#### Thermal analysis

The thermal stability of the complexes with ligand was investigated using thermogravimetric analyses (TGA). TGA was carried out at heating rate of  $10 \text{ }^\circ\text{C}/\text{min}$  in nitrogen atmosphere over a temperature range of  $25\text{--}800 \text{ }^\circ\text{C}$ . The thermogram of the complexes of Cu(II) and Ni(II) did not show any peak below  $150 \text{ }^\circ\text{C}$  which indicated that there was no water molecule inside or outside the coordination sphere. On heating, Cu(II), and Ni(II) metal complexes decomposed in three steps. First step was due to decomposition of coordinated anion at temperature  $220 \text{ }^\circ\text{C}$ . Second and third step indicated decomposition of organic moieties i.e. ( $-\text{C}_{12}\text{H}_{10}$ ) and ( $-\text{C}_4\text{H}_2\text{N}_6\text{S}_4$ ) Fig. 6(a)–(c) Table 5.

#### Molecular modeling

Because the single crystals could not be obtained for ligand and its metal complexes, it was thought worthwhile to obtain structural information. Geometry optimization was done by using Hyperchem. 7.51 version for ligand(L), [Cu(L)Cl<sub>2</sub>], [Ni(L)Cl<sub>2</sub>], and [Ni(L)](NO<sub>3</sub>)<sub>2</sub> complexes Fig. 7 (Supplementary Material). In case of ligand it was noticed that the bond length for C=N is  $1.3493 \text{ \AA}$ , C–S is  $1.8151 \text{ \AA}$  and bond angle for C=N is  $118.23^\circ$ , C–S is  $91.83^\circ$ . [Cu(L)Cl<sub>2</sub>] metal complex had tetragonal geometry, while [Ni(L)Cl<sub>2</sub>] and [Ni(L)](NO<sub>3</sub>)<sub>2</sub> complexes possessed octahedral, and tetrahedral geometry, respectively. In case of chloride complexes two axial positions were occupied by chloride ions, while

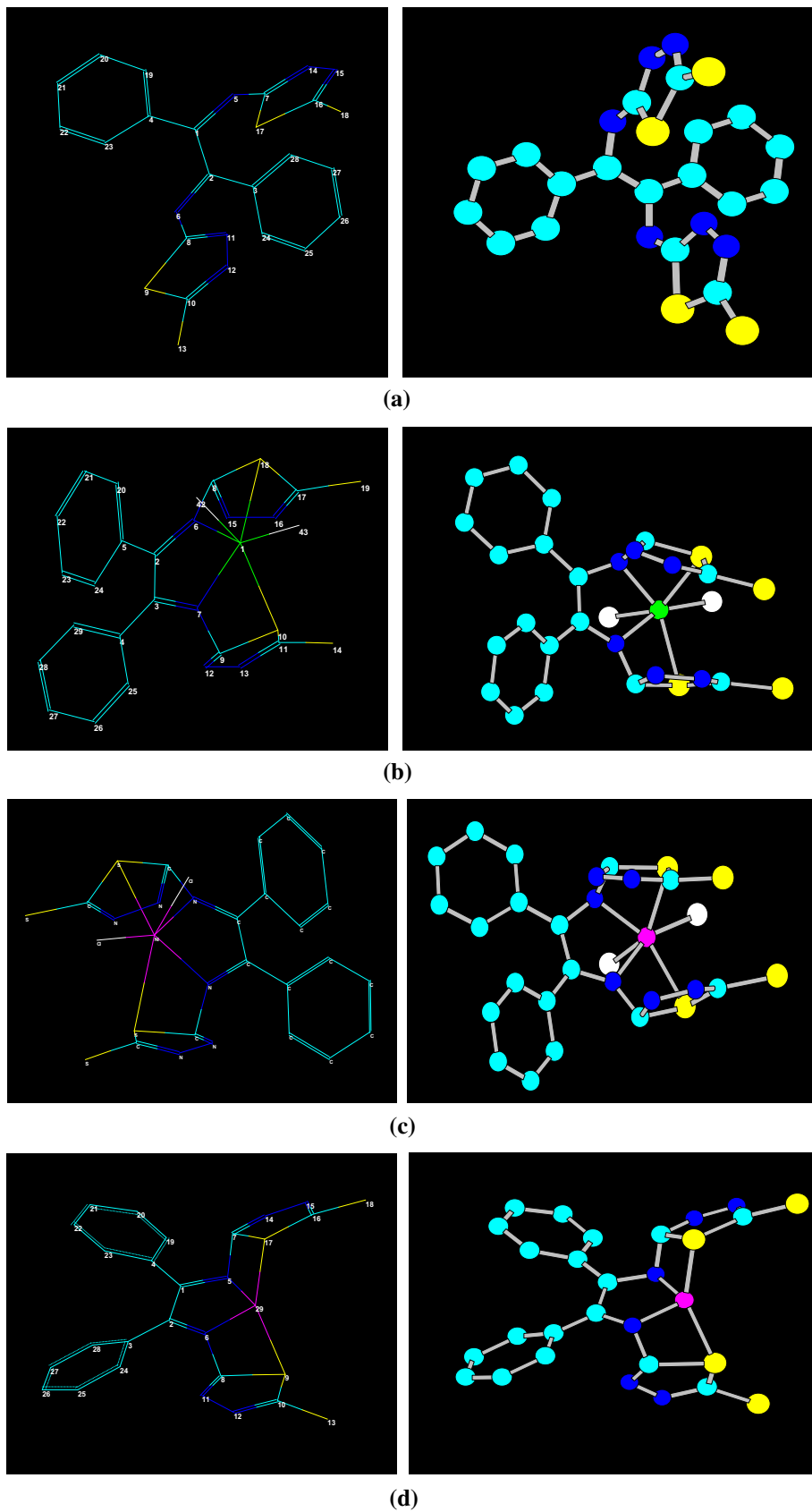


**Fig. 7.** Geometry optimized structure of (a) Schiff's base Ligand, (b)  $[\text{Cu}(\text{L})\text{Cl}_2]$ , (c)  $[\text{Ni}(\text{L})\text{Cl}_2]$  and (d)  $[\text{Ni}(\text{L})](\text{NO}_3)_2$ , [color code: C-sky blue, N-blue, S-yellow, Cu-green, Ni-pink, Cl-white]. (For interpretation of the references to color in this figure legend, the reader is referred to the web version of this article.)

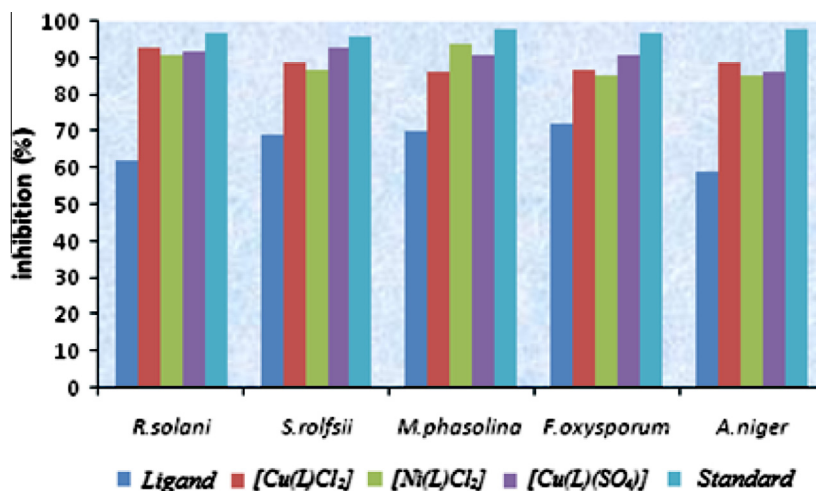


Fig. 8. Graph showing antipathogenic behavior of compounds against *R. solani*, *S. rolfsii*, *M. phaseolina*, *F. oxysporum*, and *A. niger* at concentration 200 ppm.

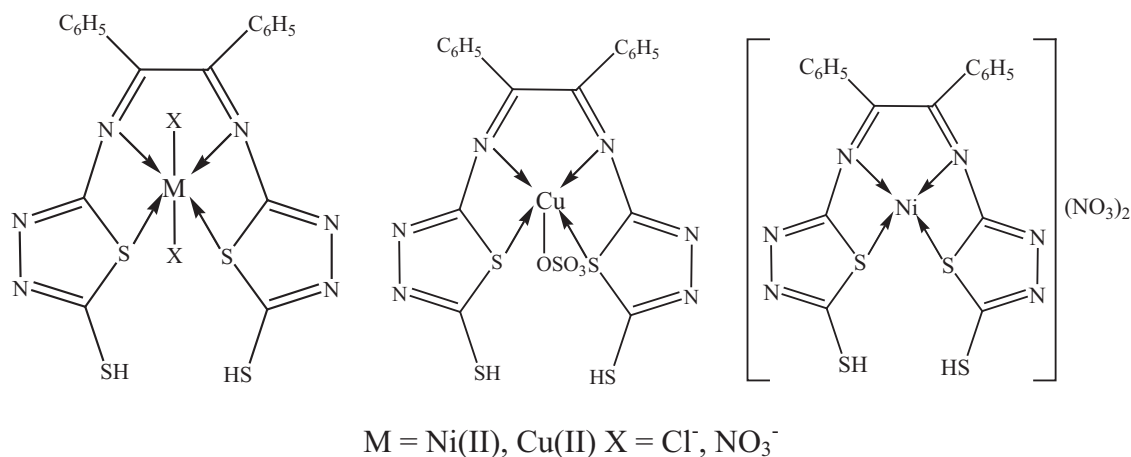
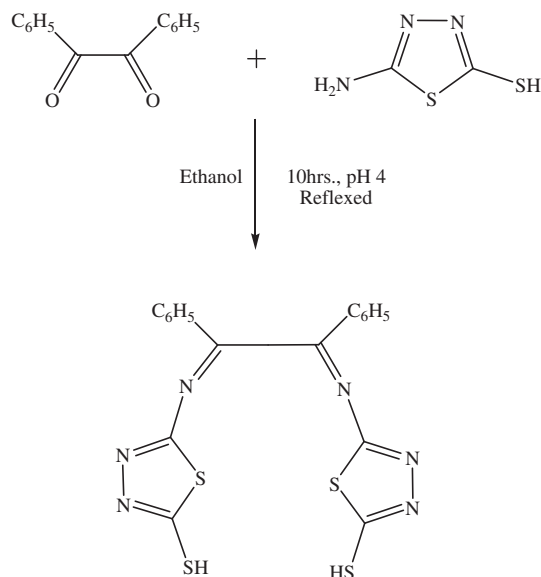


Fig. 9. Proposed structure of metal complexes.



Scheme 1. Syntheses of Schiff's base ligand benzil bis(5-amino-1,3,4-thiadiazole-2-thiol).

equatorial positions by nitrogen (C=N) and sulfur (thiol ring) atoms of the ligand. In  $[\text{Cu(L)Cl}_2]$  two equatorial Cu–N distances were 1.874 Å, 1.9011 Å and Cu–S distances were 2.2441 Å, 2.2414 Å. In  $[\text{Ni(L)Cl}_2]$  two equatorial Ni–N distances were 1.856, 1.884 and Ni–S distances are 1.355 Å, 2.231 Å, while in case of  $[\text{Ni(L)}](\text{NO}_3)_2$  two equatorial Ni–N distances were 1.784, 1.788 and Ni–S distances were 2.144 Å, 2.160 Å. The important bond angles and bond distances are summarized in Tables 6 and 7. Attempts to optimize the sulfate complexes of Cu(II) was done but attempts were found unsuccessful.

#### Antimicrobial activity

The antimicrobial activity of ligand and its metal complexes  $[\text{Cu(L)Cl}_2]$ ,  $[\text{Cu(L)(SO}_4)]$ , and  $[\text{Ni(L)Cl}_2]$  were examined. A comparative study of the growth inhibition zone values of ligand and its metal complexes indicated that metal complexes exhibited higher activity than the free ligand and the same was indicated from the results, given in Tables 8 and 9. Higher activity of metal complex was probably due greater lipophilic nature of the complex. It increased activity of the metal complex, and can be explained on the basis of Overtone's concept and Tweedy's chelation theory [26,27]. According to Overtone's concept of cell permeability, the

**Table 6**

Optimized geometry of the Schiff's base ligand and metal complexes (bond angles in degrees).

Atoms Schiff's base ligand(L)	Bond angle
C <sub>1</sub> –N <sub>5</sub> –C <sub>7</sub>	118.23
C <sub>7</sub> –S <sub>17</sub> –C <sub>16</sub>	91.83
C <sub>2</sub> –N <sub>6</sub> –C <sub>8</sub>	115.83
C <sub>8</sub> –S <sub>9</sub> –C <sub>10</sub>	91.64
<i>[Cu(L)Cl<sub>2</sub>]</i>	
S <sub>18</sub> –Cu <sub>1</sub> –Cl <sub>43</sub>	89.049
Cl <sub>43</sub> –Cu <sub>1</sub> –S <sub>10</sub>	84.142
Cl <sub>42</sub> –Cu <sub>1</sub> –N <sub>6</sub>	86.188
Cl <sub>42</sub> –Cu <sub>1</sub> –N <sub>7</sub>	85.532
N <sub>7</sub> –Cu <sub>1</sub> –S <sub>10</sub>	71.339
N <sub>6</sub> –Cu <sub>1</sub> –S <sub>10</sub>	68.636
Cl <sub>42</sub> –Cu <sub>1</sub> –Cl <sub>43</sub>	85.461
N <sub>6</sub> –Cu <sub>1</sub> –S <sub>10</sub>	116.2
N <sub>7</sub> –Cu <sub>1</sub> –S <sub>18</sub>	145.795
C <sub>2</sub> –N <sub>6</sub> –C <sub>8</sub>	126.135
C <sub>3</sub> –N <sub>7</sub> –C <sub>9</sub>	108.721
C <sub>8</sub> –S <sub>18</sub> –C <sub>17</sub>	89.306
C <sub>9</sub> –S <sub>10</sub> –C <sub>11</sub>	85.736
<i>[Ni(L)Cl<sub>2</sub>]</i>	
Cl <sub>43</sub> –Ni <sub>1</sub> –Cl <sub>42</sub>	85.45
S <sub>18</sub> –Ni <sub>1</sub> –N <sub>7</sub>	147.03
S <sub>10</sub> –Ni <sub>1</sub> –N <sub>6</sub>	114.89
Cl <sub>42</sub> –Ni <sub>1</sub> –N <sub>6</sub>	86.27
S <sub>10</sub> –Ni <sub>1</sub> –N <sub>7</sub>	71.95
Cl <sub>43</sub> –Ni <sub>1</sub> –S <sub>18</sub>	89.61
C <sub>8</sub> –S <sub>18</sub> –C <sub>17</sub>	89.23
C <sub>11</sub> –S <sub>10</sub> –C <sub>9</sub>	85.61
C <sub>9</sub> –N <sub>7</sub> –C <sub>3</sub>	108.21
C <sub>8</sub> –N <sub>6</sub> –C <sub>2</sub>	126.74
<i>[Ni(L)](NO<sub>3</sub>)<sub>2</sub></i>	
S <sub>17</sub> –Ni <sub>29</sub> –S <sub>9</sub>	137.27
S <sub>17</sub> –Ni <sub>29</sub> –N <sub>5</sub>	89.80
N <sub>5</sub> –Ni <sub>29</sub> –N <sub>6</sub>	95.57
N <sub>6</sub> –Ni <sub>29</sub> –S <sub>9</sub>	83.20
C <sub>7</sub> –S <sub>17</sub> –Ni <sub>29</sub>	67.61
Ni <sub>29</sub> –N <sub>5</sub> –C <sub>1</sub>	103.39
Ni <sub>29</sub> –N <sub>6</sub> –C <sub>2</sub>	104.75
Ni <sub>29</sub> –N <sub>6</sub> –C <sub>8</sub>	90.61
N <sub>6</sub> –C <sub>8</sub> –S <sub>9</sub>	109.14
C <sub>8</sub> –S <sub>9</sub> –C <sub>10</sub>	83.71
C <sub>4</sub> –C <sub>1</sub> –C <sub>2</sub>	127.83
C <sub>2</sub> –N <sub>6</sub> –C <sub>8</sub>	107.58

lipid membrane that surrounds the cell favors the passage of only lipid soluble materials due to which liposolubility was considered to be an important factor that controls the antimicrobial activity. On chelation, the polarity of the metal ion will be reduced to a greater extent due to the overlap of the ligand orbital and partial sharing of positive charge of metal ion with donor groups [28,29]. Further, it increases the delocalization of the  $\pi$  electrons over the whole chelate ring and enhances the lipophilicity of the complex. This increased lipophilicity enhances the penetration of the complexes into lipid membrane and thus blocks the metal binding sites on enzymes of micro organisms [30]. These metal complexes also disturb the respiration process of the cell and thus block the synthesis of proteins, which restricts further growth of the organism [31].

#### Antibacterial screening

Antibacterial activity was tested *in vitro* against *E. coli*, *S. aureus*, *P. aeruginosa*, and *K. pneumonia*. The compounds were tested at the concentration 200 ppm, 100 ppm, 50 ppm, 25 ppm, and 12.5 ppm. Table 8 indicates that [Cu(L)(SO<sub>4</sub>)] complex showed better activity against *E. coli*, *P. aeruginosa*, and *K. pneumonia* than other

**Table 7**

Optimized geometry of the Schiff's base ligand and metal complexes (bond lengths in Angstroms).

Atoms Schiff's base ligand(L)	Bond length
C <sub>1</sub> –N <sub>5</sub>	1.3493
N <sub>5</sub> –C <sub>7</sub>	1.3447
C <sub>7</sub> –S <sub>17</sub>	1.3223
S <sub>17</sub> –C <sub>16</sub>	1.8151
C <sub>2</sub> –N <sub>6</sub>	1.3497
N <sub>6</sub> –C <sub>8</sub>	1.3434
C <sub>8</sub> –S <sub>9</sub>	1.3197
S <sub>9</sub> –C <sub>10</sub>	1.8161
<i>[Cu(L)Cl<sub>2</sub>]</i>	
S <sub>18</sub> –Cu <sub>1</sub>	2.2441
Cu <sub>1</sub> –Cl <sub>43</sub>	2.2043
Cu <sub>1</sub> –S <sub>10</sub>	2.2414
Cl <sub>42</sub> –Cu <sub>1</sub>	2.2038
Cu <sub>1</sub> –N <sub>6</sub>	1.874
Cu <sub>1</sub> –N <sub>7</sub>	1.9011
C <sub>9</sub> –S <sub>10</sub>	1.745
S <sub>10</sub> –C <sub>11</sub>	1.7519
C <sub>8</sub> –S <sub>18</sub>	1.761
<i>[Ni(L)Cl<sub>2</sub>]</i>	
Cl <sub>43</sub> –Ni <sub>1</sub>	2.188
Cl <sub>42</sub> –Ni <sub>1</sub>	2.188
S <sub>10</sub> –Ni <sub>1</sub>	2.231
Ni <sub>1</sub> –N <sub>7</sub>	1.884
Ni <sub>1</sub> –N <sub>6</sub>	1.856
Ni <sub>1</sub> –S <sub>18</sub>	1.355
C <sub>8</sub> –S <sub>18</sub>	1.761
S <sub>18</sub> –C <sub>17</sub>	1.740
C <sub>11</sub> –S <sub>10</sub>	1.745
S <sub>10</sub> –C <sub>9</sub>	1.751
C <sub>9</sub> –N <sub>7</sub>	1.346
N <sub>7</sub> –C <sub>3</sub>	1.363
C <sub>8</sub> –N <sub>6</sub>	1.340
N <sub>6</sub> –C <sub>2</sub>	1.34
<i>[Ni(L)](NO<sub>3</sub>)<sub>2</sub></i>	
S <sub>17</sub> –Ni <sub>29</sub>	2.144
Ni <sub>29</sub> –S <sub>9</sub>	2.160
Ni <sub>29</sub> –N <sub>5</sub>	1.784
Ni <sub>29</sub> –N <sub>6</sub>	1.788
C <sub>7</sub> –S <sub>17</sub>	1.981
N <sub>5</sub> –C <sub>1</sub>	1.375
N <sub>6</sub> –C <sub>2</sub>	1.370
N <sub>6</sub> –C <sub>8</sub>	1.372
C <sub>8</sub> –S <sub>9</sub>	1.846
S <sub>9</sub> –C <sub>10</sub>	1.750
C <sub>4</sub> –C <sub>1</sub>	1.357
C <sub>1</sub> –C <sub>2</sub>	1.374
C <sub>2</sub> –N <sub>6</sub>	1.375

complexes and parent ligand. The order of antibacterial activity was found in order:

against *E. coli*  
 Standard > [Cu(L)(SO<sub>4</sub>)] > [Ni(L)Cl<sub>2</sub>] > [Cu(L)Cl<sub>2</sub>] > ligand  
 against *S. aureus*  
 Standard > [Ni(L)Cl<sub>2</sub>] > [Cu(L)(SO<sub>4</sub>)] > [Cu(L)Cl<sub>2</sub>] > ligand  
 against *P. aeruginosa*  
 Standard > [Cu(L)(SO<sub>4</sub>)] > [Cu(L)Cl<sub>2</sub>] > [Ni(L)Cl<sub>2</sub>] > ligand  
 against *K. pneumonia*  
 Standard > [Cu(L)(SO<sub>4</sub>)] > ligand > [Ni(L)Cl<sub>2</sub>] > [Cu(L)Cl<sub>2</sub>]

#### Antifungal screening

For fungicidal activity, compounds were screened *in vitro* against *R. solani*, *S. rolfisii*, *M. phaseolina*, *F. oxysporum*, and *A. niger*. The compounds were tested at the concentration 200 ppm, 100 ppm, 50 ppm, 25 ppm and 12.5 ppm in DMSO. From Table 9,

**Table 8**  
Antibacterial activity result of the Schiff's base ligand and its metal complexes.

Compounds	Concentration (ppm)	<i>E. coli</i>	<i>S. aureus</i>	<i>P. aeruginosa</i>	<i>K. pneumonia</i>	MIC
Ligand(L)	200	19	20	22	25	200
	100	17	17	19	22	
	50	15	13	14	19	
	25	–	09	10	14	
	12.5	–	05	06	11	
[Cu(L)Cl <sub>2</sub> ]	200	23	22	24	19	50
	100	21	19	21	17	
	50	19	17	18	14	
	25	16	14	16	11	
	12.5	14	11	14	07	
[Cu(L)(SO <sub>4</sub> )]	200	29	27	30	30	25
	100	26	24	27	27	
	50	21	20	23	25	
	25	17	16	20	21	
	12.5	15	13	19	19	
[Ni(L)Cl <sub>2</sub> ]	200	27	28	23	23	50
	100	23	25	21	21	
	50	20	23	19	19	
	25	17	19	15	16	
	12.5	13	15	13	14	
Standard (Gentamycin)	200	32	35	39	32	12.5
	100	31	33	34	30	
	50	30	30	32	29	
	25	30	28	30	27	
	12.5	30	28	30	27	

**Table 9**  
Antifungal activity result of the Schiff's base ligand and its metal complexes.

Compounds	Concentration (ppm)	<i>R. solani</i>	<i>R. rofsii</i>	<i>M. phaseolina</i>	<i>F. oxysporum</i>	<i>A. niger</i>
Ligand(L)	200	62	69	70	72	59
	100	51	57	62	63	47
	50	42	44	57	57	40
	25	33	38	48	49	29
	12.5	23	25	39	39	15
[Cu(L)Cl <sub>2</sub> ]	200	93	89	86	87	89
	100	89	73	79	79	74
	50	74	53	67	66	59
	25	65	47	43	46	42
	12.5	47	35	32	38	29
[Cu(L)(SO <sub>4</sub> )]	200	92	93	91	91	86
	100	84	88	88	86	77
	50	79	76	72	78	62
	25	59	69	59	44	57
	12.5	48	47	41	30	41
[Ni(L)Cl <sub>2</sub> ]	200	91	87	94	85	85
	100	82	72	89	79	73
	50	76	67	69	64	67
	25	65	53	58	47	53
	12.5	58	39	34	36	38
Standard (Fluconazole)	200	97	96	98	97	98
	100	93	87	91	92	93
	50	86	81	86	85	87
	25	79	73	78	78	79
	12.5	74	69	67	69	68

it was clear that the [Cu(L)(SO<sub>4</sub>)] complex shows good activity against *S. rofsii*, *M. phaseolina*, and *A. niger* Fig. 8 (Supplementary Material).

Order of antifungal activity was found in order:

against *R. solani*

Standard > [Cu(L)Cl<sub>2</sub>] > [Cu(L)(SO<sub>4</sub>)] > [Ni(L)Cl<sub>2</sub>] > ligand  
against *S. rofsii*

Standard > [Cu(L)(SO<sub>4</sub>)] > [Cu(L)Cl<sub>2</sub>] > [Ni(L)Cl<sub>2</sub>] > ligand  
against *M. phaseolina*

Standard > [Cu(L)(SO<sub>4</sub>)] > [Ni(L)Cl<sub>2</sub>] > [Cu(L)Cl<sub>2</sub>] > ligand  
against *F. oxysporum*

Standard > [Ni(L)Cl<sub>2</sub>] > [Cu(L)(SO<sub>4</sub>)] > [Cu(L)Cl<sub>2</sub>] > ligand  
against *A. niger*

Standard > [Cu(L)(SO<sub>4</sub>)] > [Ni(L)Cl<sub>2</sub>] > [Cu(L)Cl<sub>2</sub>] > ligand

## Conclusion

On the basis of the physicochemical and spectral data, we assume that ligand behaves as tetradentate [N<sub>2</sub>S<sub>2</sub>]. In the light of

above discussed studies, we proposed octahedral geometry for  $[\text{Ni}(\text{L})\text{Cl}_2]$ , tetrahedral geometry for  $[\text{Ni}(\text{L})](\text{NO}_3)_2$ , tetragonal geometry for  $[\text{Cu}(\text{L})\text{Cl}_2]$ ,  $[\text{Cu}(\text{L})(\text{NO}_3)_2]$ , and square pyramidal geometry for  $[\text{Cu}(\text{L})(\text{SO}_4)]$  complex Fig. 9 (Supplementary Material). Thermal study revealed thermal stability of complexes. Ligand and its  $[\text{Cu}(\text{L})\text{Cl}_2]$  complex showed a moderate activity against all fungi species studied here. Among all metal complexes,  $[\text{Cu}(\text{L})(\text{SO}_4)]$  complex showed an excellent inhibition.

### Acknowledgements

The author thankful to University Grant Commission (UGC), New Delhi, India for financial assistance, USIC, University of Delhi for recording TGA, IR, CHN, IIT Bombay for recording EPR spectra, and IIT Delhi for recording NMR spectra.

### Appendix A. Supplementary material

Supplementary data associated with this article can be found, in the online version, at <http://dx.doi.org/10.1016/j.saa.2014.08.046>.

### References

- [1] Q. Wang, K.Z. Tang, W.S. Liu, Y. Tang, M.Y. Tan, J. Solid State Chem. 182 (2009) 31.
- [2] A.K. Sharma, S. Chandra, Spectrochim. Acta, Part A 103 (2013) 96.
- [3] R.M. Patil, S.R. Chaurasiya, Asian J. Chem. 20 (2008) 4615.
- [4] S. Chandra, A.K. Sharma, J. Coord. Chem. 62 (2009) 3688.
- [5] A.K. Sharma, S. Chandra, Spectrochim. Acta, Part A 81 (2011) 424.
- [6] S. Chandra, S. Bargujar, R. Nirwal, K. Qanungo, S.K. Sharma, Spectrochim. Acta, Part A 113 (2013) 164.
- [7] M.A. Neelakantan, M. Esakkiamma, S.S. Mariappan, J. Dharmaraja, T.J. Kumar, Ind. J. Pharm. Sci. 72 (2010) 216.
- [8] G.A. Bohach, D.J. Fast, R.D. Nelson, P.M. Schlievert, J. Rodes, J.P. Benhamou, A. Blei, J. Reichen, M. Rizzetto, The Textbook of Hepatology: from Basic Science to Clinical Practice, Wiley Blackwell, Oxford (UK), 2007, p. 1029.
- [9] D. Sriram, P. Yogeewari, N.S. Myneedu, V. Saraswat, Bioorg. Med. Chem. Lett. 16 (2006) 2127.
- [10] G. Cerchiaro, K. Aquilano, G. Filomeni, G. Rotilio, M.R. Ciriolo, A.M.D.C. Ferreira, J. Inorg. Biochem. 99 (2005) 1433.
- [11] N. Demirbas, S.A. Karaoglu, A. Demirbas, K. Sancak, Eur. J. Med. Chem. 39 (2004) 793.
- [12] N.A. Salih, Turk. J. Chem. 32 (2008) 229.
- [13] A. Mobinikhaledi, M. Jabbarpour, A. Hamta, J. Chil. Chem. Soc. 56 (2011) 812.
- [14] H.A. Ameen, A.J. Qasir, J. Pharm. Sci. 21 (2012) 98.
- [15] A.P. Mishra, R. Mishra, R. Jain, S. Gupta, Mycobiology 40 (2012) 20.
- [16] S. Chandra, A.K. Sharma, Spectrochim. Acta, Part A 72 (2009) 851.
- [17] S. Chandra, M. Tyagi, K. Sharma, J. Iran. Chem. Soc. 6 (2009) 310.
- [18] N. Nakamoto, Infrared and Raman Spectra of Inorganic and Coordination Compounds, third ed., John Wiley & Sons, New York, NY, USA, 1978.
- [19] A.I. Vogel, A Textbook of Quantitative Inorganic Analysis, fourth ed., ELBS and Longman, 1978.
- [20] S. Chandra, A. Kumar, Spectrochim. Acta, Part A 67 (2007) 697.
- [21] S. Chandra, U. Kumar, Spectrochim. Acta, Part A 61 (2005) 219.
- [22] S. Chandra, L.K. Gupta, Spectrochim. Acta, Part A 61 (2005) 1181.
- [23] S. Chandra, L.K. Gupta, K. Gupta, J. Ind. Chem. Soc. 81 (2004) 833.
- [24] A.B.P. Lever, Crystal Field Spectra. Inorganic Electronic Spectroscopy, first ed., Elsevier, Amsterdam, 1968.
- [25] S. Chandra, K.K. Sharma, Acta Chim. Acad. Sci. Hung. Tomus 111 (1982) 5.
- [26] A.T.C. Olak, F.C. Olak, O.Z. Yesilel, D. Akduman, F. Yilmaz, M. Tümer, Inorg. Chim. Acta 363 (2010) 2149.
- [27] S. Belaid, A. Landreau, S. Djebbar, O.B. Baitich, G. Bouet, J.P. Bouchara, J. Inorg. Biochem. 102 (2008) 63.
- [28] K. Kralova, K. Kwassova, O. Svajlenova, J. Vanco, Chem. Pap. 58 (2000) 361.
- [29] J. Pwerekh, P. Inamdhar, R. Nair, S. Baluja, S. Chand, J. Serb. Chem. Soc. 70 (2005) 1161.
- [30] Y. Vaghasia, R. Nair, M. Soni, S. Baluja, S. Chand, J. Serb. Chem. Soc. 69 (2004) 991.
- [31] N. Raman, Res. J. Chem. Environ. 4 (2005) 9.